UC San Diego
UC San Diego Previously Published Works

Title
Novel states of pre-transition edge turbulence emerging from shearing mode competition

Permalink

Journal

ISSN

Authors
Miki, K
Diamond, PH

Publication Date

DOI

Novel States of Pre-Transition Edge Turbulence Emerging from Shearing Mode Competition

K. Miki[1] and P. H. Diamond[1,2]

[1] WCI Center for Fusion Theory, NFRI, Daejeon, Korea.
[2] CMTFO and CASS, UCSD, La Jolla, CA, USA.

E-mail: kmiki@nfri.re.kr

Abstract. Recent experiments have noted the coexistence of multiple shearing fields in edge turbulence, and have observed that the shearing population ratios evolve as the L-H transition is approached. A novel model including zonal flows (ZF), geodesic acoustic modes (GAM), and turbulence as a zero-dimensional self-consistent two predator- one prey system with multiple frequency shearings is proposed. ZF with finite frequency (i.e. GAM) can have different shearing dynamics from that with zero frequency, because of the finite shearing field auto-correlation times. Decomposing the broadband ZF spectrum into the two populations enables us to assign different shearing weights to the components of the shearing field. We define states with no ZF and GAM as an L-mode-like state, that with ZF and without GAM as an ZF-only state, with GAM and without ZF as GAM-only state, and both with ZF and GAM as the coexistence state. To resolve the origins of multiple shear coexistence, mode-competition effects are introduced. These originate from higher order perturbation of wave populations. The model exhibits a sequence of transitions between various states as the net driving flux increases. For some parameters, bi-stability of ZF and GAM is evident, which predicts hysteretic behavior in the turbulence intensity field during power ramp up/down studies. The presence of noise due to ambient turbulence offers a mechanism to explain the bursts and pulsations observed in the turbulence field prior to the L-H transition.

PACS numbers: 52.35.-g, 52.35.Ra, 52.25.Fi, 52.55.Fa

1. Introduction

Understanding the L-H transition requires a thorough comprehension of pre-transition turbulence [1]. It is now well established that edge turbulence has at least two constituents, namely primary modes with cause transport, and secondary shearing modes (i.e. zonal flow (ZF), geodesic acoustic mode (GAM)). The turbulence self-regulates via several shearing feedback loops. These feedback loops underpin the now familiar 'predator-prey' model structure [2]. Both GAMs and zonal flows frequently have been detected in tokamak edge turbulence [3] and have been observed to respond to changes in plasma conditions and to proximity to the L-H transition [4-6], and those driving mechanism has been theoretically and numerically studied [7-13].

 There are now many observations of changes in the relative populations (both in amplitude ratio and profile) of shearing modes, as heating power increases approaching the L-H transition [14-17]. In DIII-D experiments, it is suggested that transition from the GAM to ZF may help trigger L-H transition. Due to the change from co-injected NBI direction to balanced, an observed GAM peak in zonal flow spectrum decays and zero-mean-frequency zonal flow is established just before a sudden L-

H transition, i.e. a transition from turbulent state to a quiescent steady state in a very short time [14]. On the other hand, in ASDEX-Upgrade experiments, strong relation between GAM amplitude and the turbulence strength is observed at high q safety factor and low density, and no sign of the transition from GAM to ZF has appeared during the L-H transition [15]. This may indicate the GAM is just an easily visible secondary signature of the turbulence or may suggest a more fundamental role. In these experiments, unusual phenomena such as bursts, pulsations, etc in turbulence are observed. This is one clue that the interplay between GAM and mean flow may have an important role in the L-H transition in the edge region. Furthermore, in HL-2A experiments, a mixture of nearly zero frequency ZF and finite frequency GAM peaks is observed, which is referred as to the coexistence state [16,17], while the previous experiments, in DIII-D or ASDEX-Upgrade, shows a single significant spectrum constituent.

Taken together the observations suggest the need to understand the dynamics of GAM and ZF co-existence and mode competition, and how this competition impacts the qualitative state of edge turbulence. This directs towards the need to formulate and understand a two predators (i.e. ZF and GAM) - one prey (i.e. turbulence) model of the turbulence and transition dynamics. A simple theory is constructed to address these questions. Hence here we report on recent results from these theoretical studies. A major focus of this work is the extension of the familiar predator-prey model for shears and primary modes to treat the case of multiple predators. The model predicts new states of turbulence. In this vein, Ref. [18] discussed a multiple shearing predator-prey model, consisting of turbulence, ZF, and mean flow shear $<V_E'>$ as well. Refs. [19,20] discussed a predator-prey model associated with residual zonal flows and GAMs. This present model is an expansion of the previous one, including weights for the frequency spectrum of the shearing field. The model limits to zero-dimensional, lacking radial nonlocal effects, e.g. mode structure, flux drive, avalanches, and propagation. Though expansion to the one-dimensional model is a further goal of this study, this zero-dimensional model still yields substantial understanding regarding the origin of a GAM state and pulsations.

To address both GAM and zonal flow shears, we note that while zonal flows are stationary and exert coherent shears, GAMs oscillate and propagate radially [19], on account of polarization current effects [21]. GAM propagation thus reduces the GAM shearing efficiency, since the GAM-drift wave coherence time $\tau_{ac} = \left| \Delta q (v_{gr,GAM} - v_{gr}(k)) \right|^{-1}$ can be smaller than the ZF-drift wave coherence time.

Here Δq is the spectral bandwidth of the GAM shearing packet, $v_{gr,GAM}$ is GAM group velocity and $v_{gr}(k)$ is drift wave group velocity. This implies that a broadband GAM and ZF frequency shearing field must be characterized by *the shearing partition ratio* $\eta \equiv \tau_{ac,\omega} E_\omega / (\tau_{ac,\omega} E_\omega + \tau_{ac,0} E_0)$, where $E_{0,\omega}$ and $\tau_{ac,0,\omega}$ are the ZF and GAM energies and auto-coherence times, respectively. Note that η is set by *both* coherence times and the energies, and not simply by the ratio of shearing intensities. This issue has often been overlooked in previous analyses of the GAM's turbulence suppression effects. Note that this dynamics is comparable with the effective reduction of the time-varying $E \times B$ shearing rate [22].

The reminder of this paper is organized as follow. In Sec. 2 we introduce the minimal multiple shearing predator-prey model to describe interplay among turbulence, ZF, and GAM. In Sec. 3, we discuss why the minimal model is insufficient. Here we formulate the model with nonlinear mode competition effects. We discuss the possible stable states in the model. In Sec. 4 we briefly discuss the stability analyses for the possible fixed points. Here we find the bi-stable region of states, and thus predict the relation of the bi-stability to the hysteretic behavior of turbulence intensity and the origin of pulsations as a symptom of bistability. In Sec. 5 dynamics of the system with high q safety factor and low n density is discussed. There we introduce two main mechanisms effectively to reduce the zonal flow shearing. In Sec. 6 we conclude this paper and discuss possible implications for experiments.

2. A Minimal Multiple Shearing Predator-Prey Model.
In this section, a zero-dimensional self-consistent model to describe feedback loops between turbulence and zonal flows including geodesic curvature is introduced. Turbulence and zonal flows

have a feedback loop through shearing effects, with dynamics described by the wavekinetic equation [23]. Eigen-modes of shearing field, which are zero-frequency or finite-frequency, are defined by the fluid model [8]. Then, to describe the GAM shearing effects on turbulence together with ZF shearing, a model including the feedback loop and the fluid dynamical model is introduced. We start from the well known wavekinetic equation for drift wave action $N_k \equiv \varepsilon_k / \omega_* \propto (1 + k_\perp^2 \rho_s^2)^2 |\tilde{\phi}_k^2|$, where ω_* is drift wave frequency, and Doppler-shifted drift wave frequency $\omega_k = \omega_* + q_r U$, with respect to small-scale wave number $\underline{k}$, adiabatic coupling to the fluid ZF/GAM model which evolves flow velocity with zonal mode ($m=0$, $n=0$) $U \equiv \langle v_E \rangle$, anisotropic up-down asymmetric pressure perturbation $G \equiv \langle p \sin \theta \rangle$, and up-down anisotropic symmetric parallel velocity perturbation $V \equiv \langle v_\parallel \cos \theta \rangle$,

$$\frac{\partial N_k}{\partial t} + \frac{\partial \omega_k}{\partial \mathbf{k}} \cdot \frac{\partial N_{\mathbf{k}}}{\partial \mathbf{x}} - \frac{\partial \omega_k}{\partial \mathbf{x}} \cdot \frac{\partial N_{\mathbf{k}}}{\partial \mathbf{k}} = C\{N\}, \tag{1a}$$

$$\frac{\partial U}{\partial t} = iq_r \frac{c^2}{B^2} \int d^2\underline{k} \frac{k_\theta k_r}{(1 + k_\perp^2 \rho_s^2)^2} N_{\underline{k}} - \nu_{damp} U - \frac{2a}{n_{eq}R} G, \tag{1b}$$

$$\frac{\partial G}{\partial t} = (\frac{5}{3} + \tau)p_{eq}\frac{a}{R}U + (\frac{5}{3} + \tau)p_{eq}\frac{a}{qR}V - \gamma_{LD}G, \tag{1c}$$

$$\frac{\partial V}{\partial t} = -\frac{a}{n_{eq}qR}G + \hat{N}_{[\phi,v_\parallel]}, \tag{1d}$$

where q_r is radial wave number of zonal flow components, ρ_s is normalized Larmor radius, a and R are minor and major radius, respectively, $C\{N\}$ accounts for local-in-scale interactions of turbulence, ν_{damp} is collisional damping of zonal flow, n_{eq} and p_{eq} (and T_{eq}) are equilibrium density and pressure (and temperature) profile, respectively, τ is electron-ion temperature ratio T_e/T_i, γ_{LD} is the Landau damping rate of the GAM, and $\hat{N}_{[\phi,v_\parallel]} = -\langle [\tilde{\phi}, \tilde{v}_\parallel] \cos \theta \rangle$ is nonlinear coupling between the parallel velocity and the turbulence, which is neglected first, but the detail will be discussed in subsection 5.2. Here $[f, g] = (\partial_x f \partial_y g - \partial_x g \partial_y f)$ is Poisson bracket. Eq. (1a) is the wavekinetic equation. In Eq. (1b) the first term in the r.h.s. represents Reynolds stress, the second term is the collisional damping, and the third term is geodesic curvature term originating from a divergence of grad B drift in toroidal curvature. In Eq. (1c), the first term in the r.h.s. is a curvature drift term coupling with the zonal flow, the second term is sound wave propagation, and the third term is the Landau damping term. In Eq. (1d), the first term is the sound wave term coupling with G and the second term is the parallel nonlinear coupling term.

Now we separate wave action into mean value $\langle N_k \rangle$ and perturbation $\hat{N}_k$ with a series expansion, which associates with shearing fields the small parameter $\varepsilon \sim \omega_b \tau_{ac}$, as

$$N_k = \langle N_k \rangle + \hat{N}_k = \langle N_k \rangle + \hat{N}_k^{(1)} + \hat{N}_k^{(2)} + ..., \tag{2}$$

where $\hat{N}_k^{(m)}$ ($m=1, 2, ...$) are the m-th order perturbed action densities and ω_b is particle bounce or trapping frequency, which corresponds to the vortex circulation times in phase or eikonal space, or the shearing rate of zonal flow $\omega_b \sim q_r V_{ZF}$ or the bounce time of a trapped wave packet, whichever is shorter[1]. Using the drift wave group velocity $v_{gr} = \partial \omega_k / \partial k_r$, shearing relation $\partial \omega_k / \partial x = k_\theta U'$, we yield a mean field equation for the mean population $\langle N_k \rangle$,

$$\frac{\partial \langle N_k \rangle}{\partial t} = \sum_i \frac{\partial}{\partial k_r} \left\langle \frac{\partial \omega_k}{\partial x} \hat{N}_k^{(i)} \right\rangle. \tag{3}$$

Here we estimate an evolution of the mean wave action with quasilinear approximation. For the first order perturbed action density, assuming large-scale dependence of $\hat{N}_k^{(m)} \exp(iq_r r - i\Omega t)$, we obtain

$$\frac{\partial \hat{N}_k^{(1)}}{\partial t} = -v_{gr} \frac{\partial \hat{N}_k^{(1)}}{\partial x} + k_\theta U' \frac{\partial \langle N_k \rangle}{\partial k_r}. \tag{4}$$

Note that radial scale separation between large scale q_r and small scale k_r is consistent since $q_r \sim 1/L_n \ll k_r \sim 1/\rho_s$ is satisfied. This condition is appropriate for the edge L-mode profile. From Eq. (4), the first order wave action perturbation is described by the resonance and a slope of mean wave action spectrum as

$$\hat{N}_k^{(1)} = R(\Omega, q_r) k_\theta U' \frac{\partial \langle N_k \rangle}{\partial k_r}, \tag{5}$$

where $R(q_r, \Omega)$ is a response and can be estimated by the auto-correlation time τ_{ac} between drift wave group velocity and ZF/GAM group wave packet,

$$R(q_r, \Omega) = \iota \pi \delta(\Omega - q_r v_{gr}) \approx \tau_{ac,\Omega}. \tag{6}$$

From Eqs. (3), (5), and (6), we obtain the following quasilinear estimation,

$$\frac{\partial \langle N_k \rangle}{\partial t} = \frac{\partial}{\partial k_r} D_k \frac{\partial \langle N_k \rangle}{\partial k_r}, \tag{7a}$$

where

$$D_k = \sum_{q_r} q_r^2 k_\theta^2 \left| U_{q_r,\omega} \right|^2 \tau_{ac,\Omega,q_r}. \tag{7b}$$

Here τ_{ac,Ω,q_r} is from *Doppler-shifted* frequency dispersion $\Delta(kv - \omega_k)$ [23], which is

$$1/\tau_{ac} = \left| \Delta(kv - \omega_k) \right| = \left| (v - v_{gr}(k))\Delta k \right|. \tag{8}$$

Thus, for quasi-particles with drift wave phase velocity $v = \omega_k/k = v_{ph}$ resonating with group propagation of the GAM shearing $v_{gr,GAM} = \partial\Omega/\partial q_r = v_{ph}$, we obtain

$$\tau_{ac,\omega,q_r} \sim \left| \left(\frac{\partial\Omega}{\partial q_r} - v_{gr}(k) \right) \Delta q_r \right|^{-1}, \tag{9}$$

where Δq_r is typical width of envelope of the zonal flow and/or GAM wave packet. From Ref. [21], the averaged wave energy damping rate is estimated as

$$\gamma_{DW} = \frac{1}{\langle\varepsilon\rangle} \frac{d\langle\varepsilon\rangle}{dt} = -\frac{1}{\langle\varepsilon\rangle} \int dk \frac{2\rho_s^2 k_\theta^2}{(1 + k_\perp^2 \rho_s^2)} \sum_{q_r,\omega} q_r^2 \left| U_{q_r,\omega} \right|^2 \tau_{ac,\omega,q_r} \sigma \langle\varepsilon_k\rangle, \tag{10}$$

where $\langle\varepsilon\rangle$ is mean turbulence energy of the drift wave and $\sigma = -[k_r \partial(\omega_k \langle N_k \rangle)/\partial k_r]/(\omega_k \langle N_k \rangle)$ is characteristic of the slope in wave number of the drift wave spectrum. Here ω is to be integrated over the frequency range of GAM or ZF. Thus we treat the shearing effect as one with broadband frequency spectrum. Rewriting the mean turbulence energy as I, i.e. $I \equiv \langle\varepsilon\rangle = \int dk \omega_k \langle N_k \rangle$, we find a temporal evolution equation for turbulence energy with linear growth and nonlinear damping as well as shearing effects as

$$\frac{\partial I}{\partial t} = \gamma_L I - \Delta\omega I^2 - \sum_\omega \alpha_\omega I U_\omega^2, \tag{11}$$

where χ_L is a growth rate of turbulence intensity, which can be calculated or estimated from results of simulations or experiments by using $\chi_L = \gamma (R/L_T - R/L_{T,crit})$, where $R/L_{T,crit}$ is the linear critical temperature gradient, γ is a reference growth rate, and $\Delta\omega$ is a nonlinear damping rate of turbulence. Here $\alpha_\omega \equiv \gamma_{DW}/|U_\omega|^2 \sim \tau_{ac,qr,\omega}$ is a coupling parameter between turbulence and zonal flows related to the correlation time of the shears.

Fig. 1. A cartoon of ZF and GAM peaks from a broadband frequency spectrum.

Here we retain two different eigen-frequencies of zonal flows, i.e. *multiple frequencies*. In other words, the shearing effects are characterized by coupling of the zero frequency zonal flow shearing of $\alpha_0 I U_0^2$ and *the finite frequency GAM shearing* of $\alpha_\omega I U_\omega^2$, as illustrated in Fig. 1. Gathering the $\pm\omega$ contributions of U into the GAM shearing term, we finally obtain

$$\frac{\partial I}{\partial t} = \gamma_L I - \Delta\omega I^2 - \alpha_0 I E_0 - \alpha_\omega I E_\omega, \tag{12}$$

where $E_0 = \left| U_{q_r,0} \right|^2$ and $E_\omega = 2\left| U_{q_r,\omega} \right|^2$. Here we assume $U_{q_r,\omega_G} = U_{q_r,-\omega_G}$ for simplicity.

On the other hand, turbulence effects on zonal flow in the first term of the r.h.s. of Eq. (1b) can be written using the relation of Eq. (2) as

$$iq_r \frac{c^2}{B^2} \int d^2\underline{k} \frac{d\underline{k}k_\theta k_r}{(1+k_\perp^2\rho_s^2)^2} N_{\underline{k}} = iq_r \frac{c^2}{B^2} \int \frac{d\underline{k}k_\theta k_r}{(1+k_\perp^2\rho_s^2)^2} \sum_i \hat{N}_k^{(i)}. \tag{13}$$

Thus, taking the first order piece of the wave action in Eq. (13) and using Eqs. (5) and (6), we obtain

$$\text{Eq. (13)} \cong -q_r^2 \frac{c^2}{B^2} \int \frac{d\underline{k}k_\theta^2 k_r}{(1+k_\perp^2\rho_s^2)^2} \tau_{ac,\omega,q_r} U_\omega \frac{\partial\langle N_k\rangle}{\partial k_r} \approx +\frac{1}{2}\tau_{ac,\omega} U_\omega I, \tag{14}$$

Notice that the shearing response to the turbulence drive is sensitive to the frequency of zonal flows, via the response of the waves to the shearing field. Therefore one cannot easily determine the predator-prey coupling parameter between turbulence and ZF/GAM without decomposing the total ZFs by frequency.

Correctly to estimate the shearing response of zonal flows with multiple frequencies to turbulence, we separate U by expanding Eqs. (1b) - (1d) in Fourier frequency modes and retain the zero-frequency and the high-frequency modes. We assume that the GAM frequency exceeds the turbulence decorrelation frequency, i.e. $\omega_G \gg \gamma_L, 1/\tau_c$, but $\omega_G \ll \omega_k$ the turbulence frequency, where τ_c is turbulence decorrelation time. Thus, the GAM frequency is clearly lower than the typical drift wave frequency, so that the GAM does not violate the adiabaticity of turbulence wave action. In the event that $\omega_G < 1/\tau_c$ (quite possible at the edge), the GAM merges with the zonal flow into a net low frequency shearing field. Since $\omega_G^2 \gg \gamma_{LD}^2$ is satisfied in the edge region with $q \gg 1$, χ_{LD}^2 effects are negligible. After calculations in Appendix A, we finally obtain the following temporal evolution equation for zonal flow energy $E_0 = |U_0^2|$ and GAM energy $E_\omega = |U_{+\omega}^2| + |U_{-\omega}^2| = 2|U_\omega^2| = 2 U_{+\omega} U_{-\omega}$,

$$\frac{\partial E_0}{\partial t} = A_0(\alpha_0 I - \gamma_0)E_0, \tag{15a}$$

$$\frac{\partial E_\omega}{\partial t} = A_\omega(\alpha_\omega I - \gamma_\omega)E_\omega. \tag{15b}$$

Here the essential factors, which determine the structure of the system, are the following: (i) shearing coupling parameters $(\alpha_0, \alpha_\omega)$ which are characterized by the ZF/GAM-drift wave coherence times, $\tau_{ac,0}$
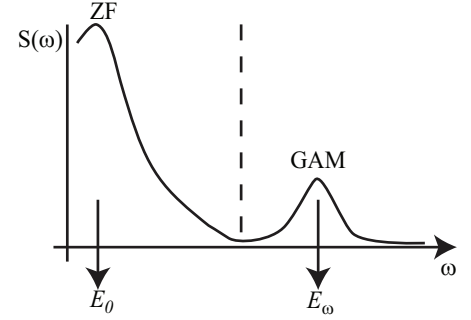
and $\tau_{ac,\omega}$, respectively (note $\tau_{ac,\omega} < \tau_{ac,0}$) (ii) the dampings of ZF and GAM, i.e. $\gamma_0 = 2\nu_{damp}$, where ν_{damp} is the collisional damping rate of ZF, and $\gamma_\omega \approx 2\nu_{damp} + 2(1+1/2q^2)\chi_{LD}$, and (iii) the screening factors regarding q-value dependency, i.e. $A_0 = (1+2q^2)^{-1}$ and $A_\omega = 1 - A_0$. Together with Eq. (12), a minimal set of self-consistent equations for turbulence, ZF, and GAM feedback loop is derived.

However we find that the minimal model cannot reproduce a state of coexistence of ZF and GAM, because the fixed point corresponding to coexistence cannot be realized. When Eqs. (15a) and (15b) are zero (fixed), at least one of two energy quantities, E_0 and E_ω should be zero. Based on the minimal model, the stability of possible states of turbulence, ZF, and GAM is investigated. Then possible nontrivial fixed points of (I, E_0, E_ω), where $\partial_t I = \partial_t E_0 = \partial_t E_\omega = 0$ are calculated. They are (i) a L-mode-like state $(I_L, 0, 0)$, (ii) a ZF-only state $(I_{0*}, E_{0*}, 0)$, and (iii) a GAM-only state $(I_{\omega*}, 0, E_{\omega*})$, where $I_L = \chi/\Delta\omega$, $I_{0*} = \gamma_0/\alpha_0$, $I_{\omega*} = \gamma_\omega/\alpha_\omega$, $E_{0*} = (1/C_0)(I_L - I_{*0})$, $E_{\omega*} = (1/C_\omega)(I_L - I_{*\omega})$, $C_0 = \alpha_0/\Delta\omega$, and $C_\omega = \alpha_\omega/\Delta\omega$. Stability analyses around the fixed points show that the smaller value of I_{*0} or $I_{*\omega}$ corresponds to the stable fixed point. Because $\gamma_0 < \gamma_\omega$ and $\alpha_0 > \alpha_\omega$ are satisfied, $I_{*0} < I_{*\omega}$ is found. Thus, the GAM-only state cannot be stabilized in this minimal model.

3. A Multiple Shearing Predator-Prey Model with Nonlinear Mode Competition.

In this section, we discuss a possible mechanism reproducing the coexistence in a multiple shearing predator-prey model. As shown in the previous section, the minimal model with only linear coupling of ZF and GAM to the turbulence cannot reproduce the coexistence. In other words, some nonlinear interaction between the predators, i.e. nonlinear *mode competition*, is necessary. The competitive exclusion principle, which forbids the stable coexistence of two or more species making their livings in identical ways, is one basic concept in ecosystem community [24]. This, then, applies to the question of ZF and GAM coexistence. Though there are many mechanisms to facilitate the mode competition, here we examine one which originates from higher order modulations of the wave actions [25, 26]. Therefore turbulence mediation is essential here. Detailed calculations are written in Appendix B. Expanding I of Eqs. (12), (15a) and (15b) in terms of E_0 and E_ω, we obtain the following multiple shearing predator-prey model with mode competition,

$$\frac{\partial I}{\partial t} = [\gamma_L - \Delta\omega I - \alpha_0 E_0(1 - \gamma_{00}E_0 - \gamma_{0\omega}E_\omega) - \alpha_\omega E_\omega(1 - \gamma_{\omega 0}E_0 - \gamma_{\omega\omega}E_\omega)]I , \qquad (16a)$$

$$\frac{\partial E_0}{\partial t} = A_0[\alpha_0 I(1 - \gamma_{00}E_0 - \gamma_{0\omega}E_\omega) - \gamma_0]E_0, \qquad (16b)$$

$$\frac{\partial E_\omega}{\partial t} = A_\omega[\alpha_\omega I(1 - \gamma_{\omega 0}E_\omega - \gamma_{\omega\omega}E_\omega) - \gamma_\omega]E_\omega, \qquad (16c)$$

where γ_{ij} $(i,j=0,\omega)$ are nonlinear coupling parameters, which can be estimated from the calculations of the higher order perturbation of wave action given in Appendix B. These are

$$\gamma_{00} \cong \frac{1}{2}\tau_{ac,ZF}^2 , \qquad (17a)$$

$$\gamma_{0\omega} \cong \frac{\tau_{ac,ZF}\tau_{ac,GAM}[(2+\varepsilon)\tau_{ac,GAM} + 3\tau_{ac,ZF}]}{4(\varepsilon\tau_{ac,GAM} + \tau_{ac,ZF})} , \qquad (17b)$$

$$\gamma_{\omega 0} \cong \frac{1}{2}\tau_{ac,GAM}^2 + \frac{1}{2}\tau_{ac,ZF}\tau_{ac,GAM} , \qquad (17c)$$

$$\gamma_{\omega\omega} \cong \frac{\tau_{ac,GAM}^2[2\tau_{ac,GAM}^2 + (2+\varepsilon)\tau_{ac,GAM}\tau_{ac,ZF} + \tau_{ac,ZF}^2]}{4(\varepsilon\tau_{ac,GAM} + \tau_{ac,ZF})} , \qquad (17d)$$

where $\tau_{ac,ZF} = \tau_{ac,q_r,0}$ and $\tau_{ac,GAM} = \tau_{ac,q_r,\omega_G}$ are autocorrelation times between drift wave group packet and ZF and GAM, respectively, and ε is a ratio of the spatial bandwidth of the GAM shearing wave packet to that of ZF shearing, $\varepsilon = \Delta q_{r,GAM}/\Delta q_{r,ZF}$.

The present model is manifestly energy conserving. For tractability we hereafter neglect the higher order terms in wave action in the turbulence intensity equation Eq. (16a). Instead we use Eq. (12) for further analyses. Essentially the higher order terms in turbulence equation are less important than those of ZF/GAM equations, because the former just correct the values of fixed points, while the latter defines the coexistence state of ZF and GAM. Though that reduced model is approximate, it still captures the essence of the dynamics of the system. Note that if we consider a model with higher order terms in the turbulence equation but without those in the ZF/GAM equations, we will lose the coexistence and also bistability shown in later analyses. More precisely, the higher order couplings in the ZF and GAM equations define the *differences* in how the ZF and GAM predators 'make their living off' of the turbulence

The system represents a generalization of the intuitively appealing predator-prey model to the case of *multiple* shearing fields with different frequencies. A state of ZF and GAM co-existence appears only when nonlinear *shearing mode competition* is included, in this case via higher order coupling through the turbulence. Our multi-predator/prey system has four nontrivial roots (fixed points: (I, E_0, E_ω)), i.e. (i) one with no shear flows (a L-mode-like state) $(I_L, 0, 0)$, (ii) a ZF-only state $(I_{0*NL}, E_{0*NL}, 0)$, (iii) a GAM-only state $(I_{\omega*NL}, 0, E_{\omega*NL})$, and (iv) a newly found *state of ZF-GAM coexistence* $(I_{*0\omega NL}, E_{0*0\omega NL}, E_{\omega*0\omega NL})$, where for $i = 0, \omega$

$$I_{*iNL} = \frac{1}{2}\left[(I_L - \Gamma_{i,s}) + \sqrt{(I_L - \Gamma_{i,s})^2 + 4\Gamma_{i,s}I_{*i}}\right],$$ (18a)

$$E_{*iNL} = \frac{1}{\gamma_{ii}}\frac{2(I_L - I_{*i})}{(I_L + \Gamma_{i,s}) + \sqrt{(I_L + \Gamma_{i,s})^2 + 4\Gamma_{i,s}(I_{*i} - I_L)}},$$ (18b)

$$I_{*0\omega NL} = \frac{1}{2}\left[(I_L - \Gamma_{0\omega}) + \sqrt{(I_L - \Gamma_{0\omega})^2 + 4(\Gamma_\omega I_{*0} + \Gamma_0 I_{*\omega})}\right],$$ (18c)

$$E_{i*0\omega NL} = \frac{1}{D}\left[\gamma_{\omega-i,\omega-i}\left(1 - \frac{I_{*i}}{I_{*0\omega NL}}\right) - \gamma_{i,\omega-i}\left(1 - \frac{I_{*\omega-i}}{I_{*0\omega NL}}\right)\right],$$ (18d)

$\Gamma_{i,s} = \alpha_i/(\gamma_{ii}\Delta\omega)$, $D = \gamma_{00}\gamma_{\omega\omega} - \gamma_{0\omega}\gamma_{\omega 0}$, $\Gamma_{ij} = C_{\omega-j}\gamma_{ij}/D$, $\Gamma_i = \Gamma_{ii} - \Gamma_{i,\omega-i}$, and $\Gamma_{0\omega} = \Gamma_0 + \Gamma_\omega$.

4. Stability analysis, bistability, and its implementation.

Here we have investigated stability of the fixed points in the multiple shearing predator-prey model with nonlinear mode competition, i.e. dynamical system analysis [27]. Keeping in mind $\partial \vec{f}/\partial t = 0$ in fixed points where $\vec{f} = (I, E_0, E_\omega)$, we solve the following eigenvalue problem for perturbations $\vec{\delta f}$ around a given fixed point $(\overline{I}, \overline{E}_0, \overline{E}_\omega)$,

$$\frac{\partial \vec{\delta f}}{\partial t} = M\vec{\delta f},$$ (19a)

where M is the dynamical matrix, with components $M_{ij} = \partial(\partial f_i/\partial t)/\partial f_j$ which are

Table 1. A table of stability conditions for the nontrivial states in collisionless case, $\gamma_0=0$. Cartoons for stability state regions as a function of $I_L(\gamma_L)$ are attached below each list. The horizontal lines show the degree of I_L, while the vertical positions in the cartoons show variation of states (ZF-only, GAM-only, and coexistence states, from top to bottom.) Note that as the margins of blocks of coexistence state drawn with dashed lines mean that to establish the coexistence state further condition: $a_0>0$ is needed.

	$\gamma_{\omega0}-\gamma_{00}>0$	$\gamma_{\omega0}-\gamma_{00}<0$	
$\gamma_{0\omega}-\gamma_{\omega\omega}>0$	(i) $D<0$ ($\Gamma_{E\omega}<0<\Gamma_{E0}$) ZF-only: $I_L>0$ GAM-only: $I_L>\Gamma_{E\omega}+\Gamma_{\omega,s}$ Coex.: $I_L>\Gamma_{E\omega}+\Gamma_{0\omega}$	(ii) $D>0$ ($0<\Gamma_{E0}<\Gamma_{E\omega}$) ZF-only: $I_L<\Gamma_{E0}+\Gamma_{0,s}$ GAM-only: $I_L>\Gamma_{E\omega}+\Gamma_{\omega,s}$ Coex.: $\Gamma_{E0}+\Gamma_{0\omega}<I_L$ $<\Gamma_{E\omega}+\Gamma_{0\omega}$	(iii) $D<0$ ($0<\Gamma_{E\omega}<\Gamma_{E0}$) ZF-only: $I_L<\Gamma_{E0}+\Gamma_{0,s}$ GAM-only: $I_L>\Gamma_{E\omega}+\Gamma_{\omega,s}$ Coex.: $\Gamma_{E0}+\Gamma_{0\omega}<I_L$ $<\Gamma_{E\omega}+\Gamma_{0\omega}$
	ZF-only state GAM-only state coexistence state $\longrightarrow I_L(\gamma_L)$	ZF-only GAM-only coex $\longrightarrow I_L(\gamma_L)$	ZF-only state GAM-only state coex $\longrightarrow I_L(\gamma_L)$
$\gamma_{0\omega}-\gamma_{\omega\omega}<0$	(iv) any D (Γ_{E0}, $\Gamma_{E\omega}<0$) ZF-only: $I_L>0$ GAM-only: undefined Coex.: undefined ZF-only state $\longrightarrow I_L(\gamma_L)$	(v) $D>0$ ($\Gamma_{E\omega}<0<\Gamma_{E0}$) ZF-only: $I_L<\Gamma_{E0}+\Gamma_{0,s}$ GAM-only: undefined Coex.: $I_L>\Gamma_{E0}+\Gamma_{0\omega}$ ZF-only coexistence state $\longrightarrow I_L(\gamma_L)$	

$$M=\begin{pmatrix} -\Delta\omega\bar{I} & -\alpha_0\bar{I} & -\alpha_\omega\bar{I} \\ \dfrac{\gamma_0 A_0\bar{E}_0}{\bar{I}} & \begin{bmatrix} -A_0\alpha_0\gamma_{00}\bar{I}\bar{E}_0 & (\bar{E}_0\neq0) \\ A_0[\alpha_0\bar{I}(1-\gamma_{0\omega}\bar{E}_0)-\gamma_0] & (\bar{E}_0=0) \end{bmatrix} & -A_0\alpha_0\gamma_{0\omega}\bar{E}_0\bar{I} \\ \dfrac{\gamma_\omega A_\omega\bar{E}_\omega}{\bar{I}} & -A_\omega\alpha_\omega\gamma_{\omega0}\bar{E}_\omega\bar{I} & \begin{bmatrix} -A_\omega\alpha_\omega\gamma_{\omega\omega}\bar{E}_\omega\bar{I} & (\bar{E}_\omega\neq0) \\ A_\omega[\alpha_\omega\bar{I}(1-\gamma_{\omega0}\bar{E}_0)-\gamma_\omega] & (\bar{E}_\omega=0) \end{bmatrix} \end{pmatrix}.$$

(19b)

Stability of the various states and their parameter dependency is examined in the collisionless case $\gamma_0=0$ as summarized in Table 1. Here $\Gamma_{E0}=(\gamma_{00}I_{*\omega}-\gamma_{\omega0}I_{*0})/(\gamma_{00}-\gamma_{\omega0})$, $\Gamma_{E\omega}=(\gamma_{0\omega}I_{*\omega}-\gamma_{\omega\omega}I_{*0})/(\gamma_{0\omega}-\gamma_{\omega\omega})$, and

$$a_0=\alpha_0\alpha_\omega\Delta\omega D\bar{I}^2+[\alpha_0\alpha_\omega(\gamma_0\gamma_{\omega\omega}+\alpha_\omega\gamma_{00})-(\alpha_\omega^2\gamma_0\gamma_{\omega0}+\alpha_0^2\gamma_\omega\gamma_{0\omega})]. \tag{20}$$

Cartoons in Table 1 exhibits possible transitions or overlaps of stable states as the drive $I_L(\gamma_L)$ increases. However we note that depending on the nonlinear coupling parameters, how states overlap for a given assumed power level is still arbitrary.

The conditions of the stability of each state are estimated by the following arguments. The fixed points, corresponding to the ZF-only, the GAM-only, and the coexistence states, are substituted into the dynamical matrix M of Eq. (19b). Then three eigenvalues of each state are obtained. To identify a
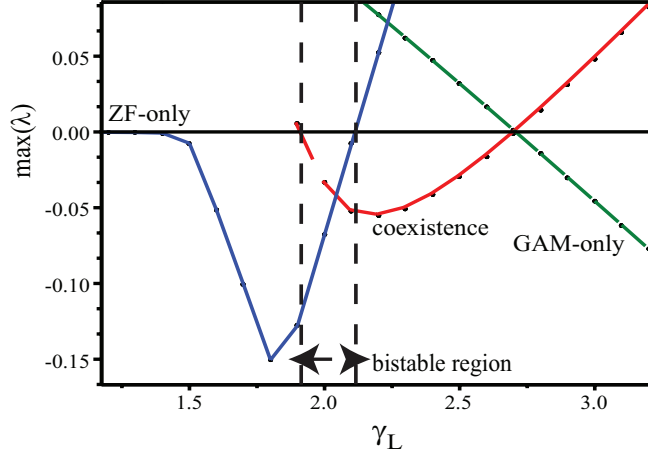
Fig. 2. Temperature gradient (γ_L) scan of maximum eigenvalues(growth rate) λ for the various equilibrium states. In the region $1.9<\gamma_L<2.1$, both ZF-only and the coexisting state are stable, thus establishing bistability.
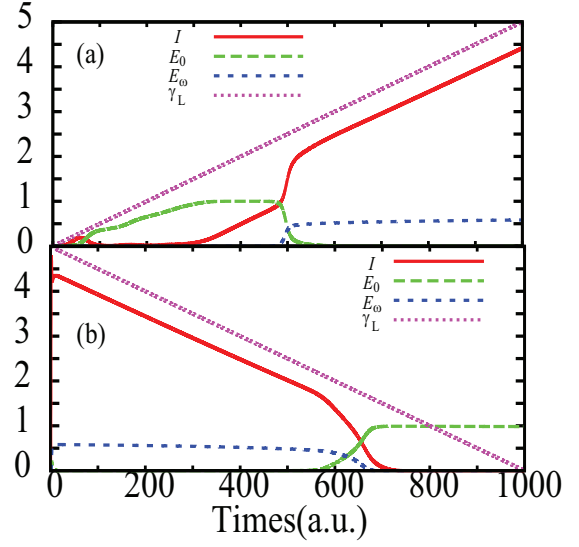

Fig. 3. Time evolution of I, E_0, E_ω, with artificial (a) increasing $\gamma_L(L_T^{-1})$ and (b) decreasing γ_L (L_T^{-1}).
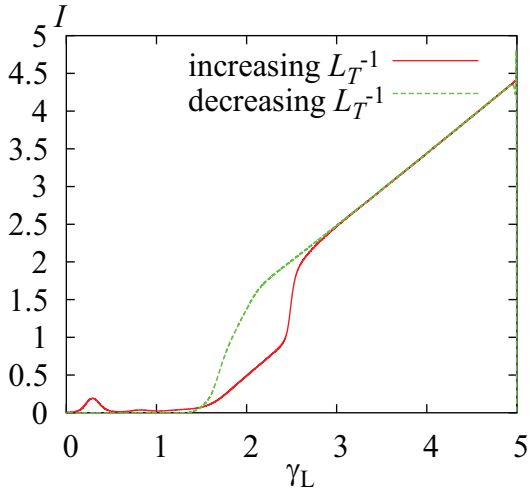

Fig. 4. Plots of evolution of turbulence intensity I versus temperature gradient (γ_L) in cases with induced ramp up/down of L_T^{-1}.
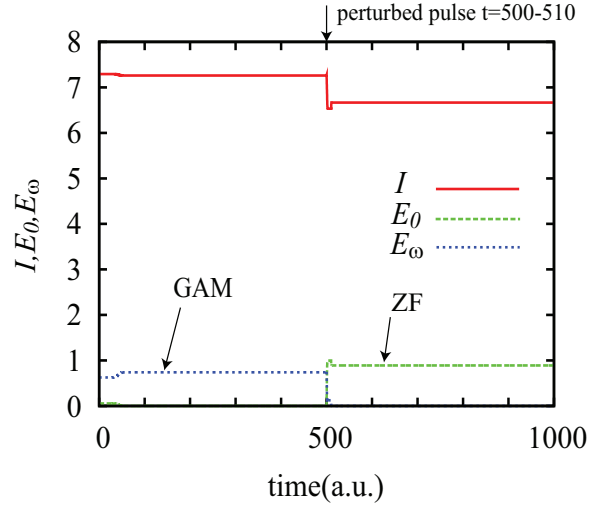

Fig.5. Temporal evolution of I, E_0 and E_ω with parameters as a bistability of ZF-only and GAM-only states is established. At t=500-510, external noise is applied to turbulence field.

state as structurally stable, all real part of the eigenvalues must be negative, i.e. max(λ_i)<0, where λ_i is the real part of eigenvalues (i=1,2,3). Furthermore, E_0, E_ω>0 are necessary due to physical limitations. Here we simplify conditions with $I_{*iNL}\sim I_L$-$\Gamma_{i,s}$ assuming I_L>>$\Gamma_{i,s}$. The estimation is consistent with the numerical tests shown next. Regarding the coexistence state, the stability conditions are estimated from both the physical limitation of the positive ZF and GAM energy population and the Routh-Hurwitz stability criterion. Here the criterion can be reduced to the condition of a_0>0 in Eq. (20).

A numerical survey of the model reveals a sequence of transitions between various roots as the driving flux, or equivalently, while $\chi_L(R/L_T-R/L_{T,crit})$, increases. The precise sequence of states varies

with system parameters (i.e. γ_{ij}). First we investigate a case with the following parameters: γ_{00}=1.0, $\gamma_{0\omega}$=2.0, $\gamma_{\omega 0}$=0.1, and $\gamma_{\omega\omega}$=1.5, (and thus γ_{00}-$\gamma_{\omega 0}$>0, $\gamma_{0\omega}$−$\gamma_{\omega\omega}$>0, and D>0). The other parameters are α_0=1.5, α_ω=1.0, γ_{damp}=10^{-4}, q=1.0, and χ_D = 1.0·exp(-q^2). Figure 2 shows a sequence of transitions between ZF-only, GAM-only, and coexistence states with these parameters. Here the vertical axis represents the maximum of eigenvalues around corresponding fixed points, and thus the positive value shows unstable region, while the negative one shows stable. We find that the ZF-only state is stabilized in weak turbulence region (χ_L<2.1 (a. u.)), the coexistence state occurs for the region 1.9<χ_L<2.7, and the GAM-only state is in 2.7<χ_L. This indicates the GAM's shearing proportion η tends to increase during a power ramp up, and reaches 1 in some cases. Note that this picture neglect mean flow effects and thus cannot describe a transition of profile [28]. Interestingly, bi-stability is evident, i.e. for some ranges of R/L_T-$R/L_{T,crit}$ (here, 1.9<γ_L<2.2), i.e. both ZF-only (or GAM-only states) and ZF/GAM coexistence states are possible, as shown in Fig. 2.

Multiple states coexistence in turn suggests the origin of hysteretic behaviour, which is predicted for power ramp up/down studies. Here we have compared cases with increasing and decreasing L_T^{-1}, as seen in Fig. 3. In Fig. 3(a), as power ramps up, a transition of states from the ZF-only to the GAM-only state through coexistence is seen at χ_L~2.5, where a bifurcation from the coexisting to the GAM-only state is seen in Fig. 2. On the other hand, in Fig. 3 (b), as power ramps down, the transition from the GAM-only state to the ZF-only state is found through the coexisting state around 2.5>γ_L>1.8, which corresponds to the region where the coexisting state is stabilized in Fig. 2.

As the behaviors of transition between the ZF-only and GAM-only states are different in Figs. 3(a) and 3(b), behaviors of turbulence level are also different. Now we plot these evolutions of turbulence intensity I versus χ_L in Fig. 4. We find hysteretic behavior of turbulence intensity I there. Note that we find a criterion that the bistability is established, i.e. α_ω/α_0<$\gamma_{0\omega}/\gamma_{00}$. The bistability in the shear field of low frequency and high frequency ZF is due to the different shearing effects, with their different coherent times, dampings and screenings.

Moreover, bistability in the presence of noise [29] (due ambient turbulence) offers a novel mechanism, to explain the bursts and pulsations [15] observed in the turbulence field prior to the L-H transition. Generally, in the bistable condition, states are determined by initial value manifolds, i.e. how close to the fixed point the initial conditions are set. That is, the bistability (and also hysteresis) are sensitive to the initial conditions and not robust (as discussed in Ref. [30].) In order that a state evolves to another, a certain amount of free energy may be necessary, in order to overcome a potential hill. The probability to transfer can be described by the classical theory of Kramers for the escape rate G from the potential well, that is

$$G \propto \exp(-\Delta V / \sigma^2),\tag{21}$$

where ΔV is related to the size of the potential well between a stable state and a transient (unstable) state and σ^2 is the variance of noise, assuming relatively small noise [31]. Fig. 5 shows an example that an artificial small perturbation can scatter states with the GAM-only to the ZF-only state. Here parameters are set as the bistability of GAM-only and ZF-only is established.

5. Discussions of high q value and low n physics

In this section we discuss possible mechanisms that the GAM-only state is stabilized in high-q safety factor regions, as often discussed in the edge simulations and experiments. Here we propose two different mechanisms to stabilize the GAM-only state, i.e. (i) the mode competition can decrease the zonal flow shearing and (ii) $v_{\|}$ nonlinearity reduces the zonal flow shearing effectively.

5.1. Mode competition effects on the zonal flow shearing

Here we discuss how the bistability is practically established by the mode competition effects. Maps of stable states as functions of two kinds of damping parameters, the collisional damping ν_{damp} and the
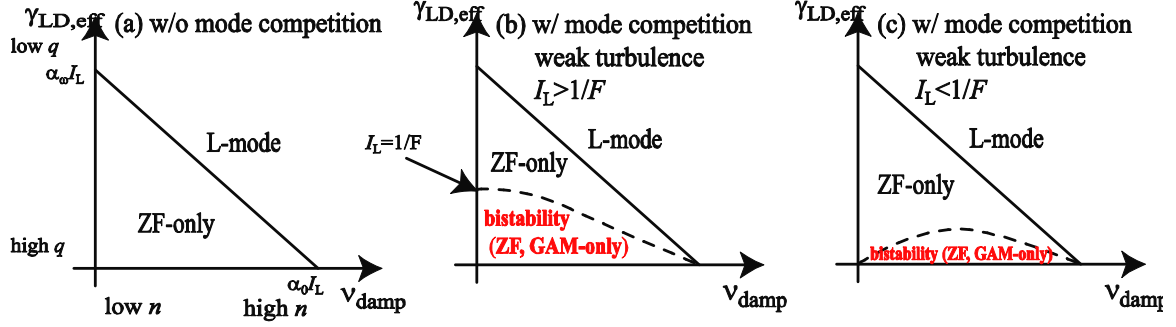
Fig. 6. Maps of stable state as functions of collisional damping ν_{damp} and effective Landau damping $\chi_{LD,eff}$ in cases (a) without the nonlinear mode competition, (b) with mode competition and assuming weak turbulence and $I_L > 1/F$, and (c) with mode competition and assuming weak turbulence and $I_L < 1/F$.

effective Landau damping $\chi_{LD,eff}(=(1+1/2q^2)\chi_D)$ are shown in Figs. 6. Low and high collisions correspond to cases with low and high density n, respectively, while low and high Landau damping correspond to cases with high and low safety factor q-value. The case of Fig. 6(a) is discussed in Sec. 3, the ZF-only state is always stabilized when $I_{*0} < I_L$, $I_{*\omega} < I_L$, (and also $I_{*0} < I_{*\omega}$) are satisfied. Then, upper critical of the collisional damping and the Landau damping rate are $\gamma_{LD,eff,crit} = \alpha_\omega I_L$ and $\nu_{damp,eff} = \alpha_0 I_L$, respectively. On the other hand, in case with the mode competition a criterion to stabilize the GAM-only state is obtained from $M_{22} < 0$ in Eq. (18b), substituting the values of the fixed point corresponding to the GAM-only state: $(I, E_0, E_\omega) = (I_{*\omega NL}, 0, E_{*\omega NL})$ (see Eqs. (18a) and (18b)), that is

$$I_{*\omega NL} - I_{*0,eff} < 0,$$ (22a)

where

$$I_{*0,eff} = \gamma_0 / \alpha_{0,eff} = \gamma_0 / [\alpha_0 (1 - \gamma_{0\omega} E_{\omega NL})].$$ (22b)

Eqs. (22a) and (22b) show that in order that the GAM-only state to be stabilized, the ZF shearing must be effectively reduced by the nonlinear mode competition caused by the GAM energy as Eq. (22a) is satisfied. On the other hand, owing to the self-suppression effect of the GAM mainly related to the factor $\gamma_{\omega\omega}$, the turbulence level of the GAM-only state $I_{*\omega NL}$ increases from that without the nonlinear mode competition $I_{*\omega}$. However, from insights from simulations [32] and experiments [15], we assume the self-suppression effect of the GAM is weak, $\gamma_{\omega\omega} \ll 1$. Thus, $I_{*\omega NL} \sim I_{*\omega}$. Using an identity $E_{*\omega NL} = (1/C_\omega)(I_L - I_{*\omega NL})$, Eq. (22a) comes

$$I_{*\omega}[I_{*\omega} - (I_L - 1/F)] < I_{*0}/F,$$ (23)

where $F = (\gamma_{0\omega}/C_\omega)$. As seen in Eq. (23), a bifurcation is found to occur when $I_L = 1/F$. Whichever in both cases of Figs. 6(b) or 6(c), a bistablily, i.e. both the ZF-only and the GAM-only states are stabilized, is found in lower Landau damping (thus high q-value) region. The upper limit of the Landau damping rate scale to occur the bistability is estimated at $\gamma_{LD,eff} \sim \alpha_\omega/F$.

5.2. $v_{//}$ nonlinearity effects on ZF/GAM shearings

The effect of $v_{//}$ nonlinearity $\hat{N}_{[\phi, v_{||}]} = -\langle [\tilde{\phi}, \tilde{v}_{||}] \cos\theta \rangle$ written in Eq. (1d) is introduced here. With aid of the Taylor identity,

$$N_{[\phi, v_\parallel]} \cong -\frac{\partial}{\partial x}\left\langle (\tilde{\phi}\frac{\partial \tilde{v}_\parallel}{\partial y})\cos\theta \right\rangle \approx -(q_r\rho_s)(k_\theta\rho_s)\left\langle \tilde{v}_m\tilde{\phi}^*_{m+1}\right\rangle, \tag{24}$$

where m is the poloidal mode number. To estimate $\left\langle \tilde{v}_m\tilde{\phi}^*_{m+1}\right\rangle$, here we compare the drift wave term $L_n^{-1}(\partial\tilde{\phi}/\partial y)$ with the grad B drift term $2R^{-1}\nabla_x\tilde{\phi}$ in the density continuity equation, assuming these terms are the same order. Then we estimate

$$\tilde{\phi}_{m+1} \sim \frac{R}{2q_r\rho_s}\frac{1}{L_n}\frac{m}{a}\rho_s\tilde{\phi}_m, \tag{25}$$

where m is poloidal mode number of the mainly excited turbulence (pump wave), L_n is characteristic length of density gradient. Next we compare the drift wave term $L_n^{-1}(\partial\tilde{\phi}/\partial y)$ with the sound wave propagation term $\nabla_\parallel\tilde{v}_\parallel$. We estimate

$$\tilde{v}_{\parallel m} \sim \frac{qR}{L_n}\frac{\rho_s}{a}\tilde{\phi}_m. \tag{26}$$

Then using Eqs. (24)- (26) and $m/a\sim k_\theta$, we obtain a quasilinear estimation of the nonlinear coupling term as

$$N_{[\phi, v_\parallel]} \sim -\int d\underline{k}\frac{q}{2}\left(\frac{R}{L_n}\right)^2(k_\theta\rho_s)^2\left(\frac{\rho_s}{a}\right)|\tilde{\phi}_k^2|$$

$$\cong -\frac{q}{2}\left(\frac{R}{L_n}\right)^2\left\langle k_\theta\rho_s\right\rangle^2\left(\frac{\rho_s}{a}\right)\frac{1}{2}\tau_{ac,\omega}U_\omega I \equiv -\frac{1}{2}b\tau_{ac,\omega}U_\omega I. \tag{27}$$

Here we have used the relation in Eqs. (13) and (14). In the same manner to obtain Eqs. (15a)- (15b), we again calculate the evolutions of ZF and GAM energy populations. The result shows a similar form as Eqs. (15a) and (15b) but has differences in the coefficients of α_0 and α_ω, which are

$$\alpha'_0 = \tau_{ac,0}(1-\sqrt{2}qb), \tag{28a}$$

$$\alpha'_\omega = \tau_{ac,\omega}(1-\frac{\sqrt{2}q}{1+2q^2}b). \tag{28b}$$

These show that the ZF shearing is effectively *decreased* by the $v_\parallel$ nonlinearity, while the GAM one stays mostly constant in high q-value. We here discuss the condition that the GAM-only state can be stabilized, i.e. $I_{*0}>I_{*w}$. Replacing α_0 and α_ω of Eqs. (15a) and (15b) with α_0' and α_ω' of Eqs. (28a) and (28b), respectively, we obtain a new condition that the GAM-only state is stabilized by the parallel velocity nonlinearity, which is

$$\frac{v_{damp}}{\tau_{ac,0}(1-\sqrt{2}qb)} > \frac{v_{damp}+(1+1/2q^2)\gamma_{LD}}{\tau_{ac,\omega}(1-\dfrac{\sqrt{2}q}{1+2q^2}b)}. \tag{29}$$

Solving Eq. (29) for q, we could obtain a critical q-value q_{crit} that the GAM-only state is stabilized instead of the ZF-only state in the minimal model. Here assuming high q and low n, i.e. $q\gg1$ and $v_{damp}\to0$, we simplify the condition Eq. (29) as

$$1-\sqrt{2}qb < 0. \tag{30}$$

Then, we estimate the critical q-value,

$$q_{crit} \sim \left(\frac{R}{L_n}\right)^{-1} \langle k_\theta \rho_s \rangle^{-1} \left(\frac{a}{\rho_s}\right)^{-1/2} \tag{31}$$

For example, applying $R/L_n \sim 2.2$, $k_\theta \rho_s \sim 1$, and a ρ_* scale $(a/\rho_s) \sim 100$, $q_{crit} \sim 5.4$, and for $(a/\rho_s) \sim 1000$, $q_{crit} \sim 17$ are estimated. Above the critical q-value, the perpendicular Reynolds stress is cancelled by the parallel nonlinear effect effectively regarding ZF energy trade-off. Therefore the ZF-only state cannot survive anymore, and then the GAM-only state can be dominant.

6. Conclusions and discussions.

We have identified possible states of ZF/GAM/turbulence based on the multiple shearing predator-prey model with mode competition. Broadband shearing is characterized by a shear coherence time as well as the shear strength. Therefore we define the shearing partition ratio $\eta \equiv \tau_{ac,\omega} E_\omega /(\tau_{ac,\omega} E_\omega + \tau_{ac,0} E_0)$, i.e. GAM and ZF shearing relative to the total (GAM+ZF) shearing. Based on the understanding of GAM and ZF shearing, we have investigated the ZF/GAM interaction and constructed a minimal predator-prey model with multiple shearings. The minimal predator-prey model consists of one prey — i.e. the $m \neq 0$, $n \neq 0$ turbulence population — and two predators, i.e. ZF with $\omega \sim 0$ and GAM with $\omega \sim \omega_{GAM}$. Since the most minimal model cannot describe the coexistence of ZF and GAM, we consider a mechanism of nonlinear mode competition via coupling through higher order wavekinetics. This model predicts four states — an L-mode-like state (no flow), a ZF-only, a GAM-only, and the coexistence states — as possible fixed points of the system. We have examined one case, and have found the sequence of states selected by power evolution and parameters. As power increases, the ZF-only state evolves to the GAM-only state through a coexistence state. This indicates that *GAM tends to be excited by stronger turbulence above the critical, while ZF is excited in the weaker turbulence state* due to the nonlinear mode competition. In other words, the "state" is established by the reduction of the ZF shearing due to the nonlinear mode competition. An ASDEX-Upgrade experimental result shows that below a certain amount of turbulent intensity (or electron temperature gradient), the GAM does not survive. (Note that these observations are for regimes of low density and high q_{95} [15].) This fact can elucidate why nonlinear mode competition is necessary for the GAM-only state to survive.

We have found that bistability in shearing field is possible and thus jumps or transition between GAM and ZF states are possible. We also predict a hysteretic behavior during power ramp up and down, which originates from the nature of bistability. The bistable property suggests the possibility for noise or pulsations to determinate the state of the system. For example, in laser experiments with a bistable system, periodic pulsations with moderate intensity can synchronize with the transition of states [31,33]. Such phenomena may be related to the GAM/mean flow dynamics seen in the ASDEX Upgrade experiments [15]. Furthermore we remark the strength of pulsations may be related to avalanche dynamics, i.e. the spectrum and probability distribution function (PDF) of heat flux and its effects on ∇T. This follows from the fact that the edge turbulence and shears will surely respond to the arrival of avalanches at the edge region. Thus, an improved model should replace local γ by heat flux decomposed into a mean (deterministic) $\langle Q \rangle$ and a fluctuating (stochastic) $\tilde{Q}$ piece. Another possible mechanism for the origin of noise is emission from smaller scales to a broadband region of larger scales. Coupling of drift waves accounts for low frequency beat modes (i.e. $\omega_{k1} - \omega_{k2}$), which drive the GAM and ZF and also broadens the pump modes. (See Fig. 7.) The disparate scale interaction often causes nonlocality or non-Gaussian behavior, in which the PDF has a long tail, often
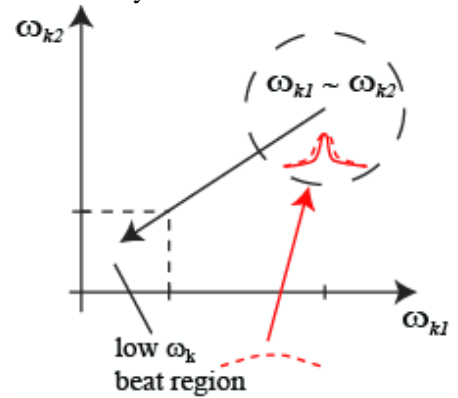
Fig. 7. A schematic cartoon of emission from smaller scales to a broadband region of large scales.

symptomatic of intermittency [34]. This intermittent turbulence behavior can appear as noise in the system. To address the question of what are critical parameters for pulsations? We note a clue is in the probability of stochastic transition of Eq. (21). That will be determined by the balance between the potential well depth, i.e. system restriction or some quantities determined by one stable state and one unstable (saddle node) state, and the variation of noise, i.e. the strength of bursts or a PDF of flux. More detail should be examined in the future.

The GAM-only state can be stabilized by two possible mechanisms. One is due to the mode competition. The bistability of the ZF-only and the GAM-only state is identified as shown in Figs. 6. These show high q-value profile also tends to establish the bistability of the ZF and GAM-only states by the nonlinear mode competition. GAM energy accumulation can affect on ZF shearing dynamics through the nonlinear mode competition, which is caused by a flattening of shearing slope. How much the nonlinear mode competition affects the bistability criterion is determined by the comparison with the GAM shearing. There, a small fluctuation can change states between the ZF-only and the GAM-only ones.

On the other hand, $v_{\parallel}$ nonlinearity effectively reduces the ZF shearing as q-value increases, while the GAM shearing mostly stays constant. Thus the ZF shearing can be lower than the GAM one in high q case, and then the GAM-only state can be stabilized instead of the ZF-only state. This mechanism is independent of the mode competition. Therefore assuming very high q-value, we expect the GAM-only state is always stabilized even without the turbulence mediation. Hereby we have found the new scale of the critical q-value, which depends on $(a/\rho_s)^{1/2}$. This indicates that the large devices such as ITER should have a higher critical q-value, so that the ZF-only state there is more easily stabilized. The state of coexistence can be also affected by q-value through Eq. (18d). Detailed comparison of them with experiments will be discussed in future works, but these tendencies are mostly consistent with experimental results.

Considering further conditions, such as the collisional damping, the Landau damping, and the turbulence intensity related to mode competition, we could identify the stability of the GAM-only state. Especially, with the mode competition, the critical q-value is down-shifted. In the large devices with low ρ_* the mode competition may be more relevant in the stabilization of the GAM state. Therefore, we remark a measurement of ambient turbulence amplitude in relation to ZF/GAM amplitudes gets more important.

Furthermore $v_{\parallel}$ dynamics could also be important in wavekinetic theory, as was done for perpendicular perturbations. Due to compressibility of GAM, GAM could have a parallel flow shearing, while ZF does not have any parallel perturbation. For the GAM shearing, a parallel Doppler shift effect can be considered in Eq. (1a) as

$$\omega_k \rightarrow \omega_{k0} + \underline{k} \cdot \underline{v} = \omega_{k0} + k_\theta \widetilde{v}_{\theta_{GAM}} + k_\parallel \widetilde{v}_{\parallel_{GAM}} \ . \tag{32}$$

However, since $k_\theta \sim 1/\rho_s >> k_{//} \sim 1/qR$, the parallel compression is negligible in tokamak plasmas. As summary, two kinds of dynamics can be considered regarding $v_{\parallel}$ nonlinearity of GAM: one is perpendicular Reynolds stress of $<v_{\parallel}\cos\theta>$, i.e. $\Pi_{v_{\parallel}\cos\theta,vr} = <v_r v_{//}\cos\theta>$, which importance is discussed in subsection 5.2, and the other is a parallel flow shearing discussed above. The former is crucial above a certain critical q-value (Eq. (31)), while the latter is not essential in the regular condition. The higher order wavekinetics regarding the $v_{\parallel}$ nonlinearity might have to be considered in such high q cases. However, because the GAM-only state is established by the $v_{\parallel}$ nonlinearity above the threshold *without mode competition*, we do not need to consider the higher order dynamics qualitatively.

Note we use terms, the "weak" or "strong turbulence". Physically they mean zonal flow self-suppression effects are manifest in the strong turbulence region, while in weak turbulence region the effect is not dominant. Therefore in the weak turbulence region, turbulence level is be estimated by the linear (minimal) model, while in the strong turbulence region the turbulence level is estimated by the nonlinear (mode competition) model. The strong turbulence region may be related to the region above the nonlinear critical gradient, i.e. Dimits shift [35].

Several thoughts for experiments are listed here:

- Fundamentally we should map toroidal mode number $n=0$ spectrum in the space of k_r and ω to measure the GAM and ZF population density. This should be mapped as a windowed function of radius to separate GAM and ZF dominated regions.
- Mapping of ambient turbulence intensity as functions of ZF and GAM amplitude can show evidence of the nonlinear mode competition due to turbulence mediation. If GAM excitation is pronounced in the region with strong turbulence intensity, turbulence mediation may be essential to GAM nonlinear excitation. Previous Landau-fluid simulations found that the ZF amplitude is constant for various temperature profiles, localized at inner region with less turbulence, while GAM intensity is correlated with the turbulence intensity and ZF is more weakly excited around the peak of turbulence where GAM amplitude has its peak (see Fig. 8 or Ref. [32]). Note that this simulation does not include mean flow. It is useful to map η as functions of Q and r. This parameter can help to characterize the importance of the GAM as a function of power ramp and radial location.
- Determination of the correlation time of the shear in ω bands as well as energies is important to estimate GAM's and ZF's contribution to shearing. As shown in Ref. [21], we have found that different shearing coefficients corresponding to coherence times between GAM/ZF-drift wave packets can be expected.
- Another goal regarding the GAM propagation is to map (k_r, ω) and then construct $\partial \omega / \partial k_r$ (i.e. GAM group velocity) contours. A survey of the group propagation of GAM as well as that of the phase propagation is helpful to understand GAM nonlocal dynamics.
- Bicoherence analysis can elucidate how the mode competition can be constructed and it might be helpful to expand our insights into the mode competition mechanism. An experimental test of the bistability or hysteresis in η in power ramp up/down is possible.
- It is useful to examine the possibility of evolution of $1/\tau_{c,turb}$ and $\omega(k)_{GAM}$ cross-over. For edge plasmas, the GAM frequency must decrease with temperature, while the turbulence has finite frequency with increasing intensity as it approaches the edge. Therefore the GAM frequency peak can be degenerate with ZF when $1/\tau_{c,turb} \sim \omega(k)_{GAM}$ is satisfied. This can be another reason why the observed GAM condenses at the edge. Therefore observation of possible cross-over is important to understand the edge turbulence/ZF/GAM interplays.

To comprehend the edge turbulence physics during the L-H transition, the following further works are needed. First we need to expand this to a one-dimensional model involving mean flow shear effects
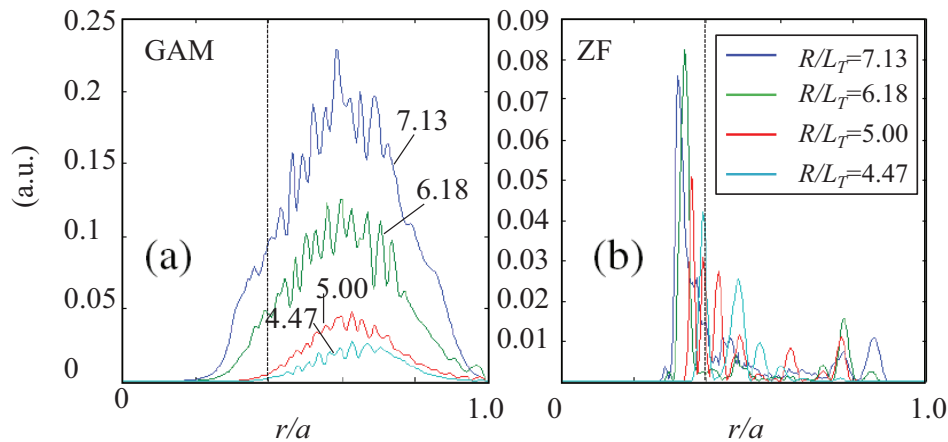

Fig. 8. Time averaged profile of (a) GAM and (b) ZF Energies with various temperature gradients in Landau-fluid simulations [32]. Vertical dotted lines denote r/a=0.4.

and GAM propagation. A more complete consideration of the mode competition mechanism is required, i.e. mean flow shear can surely affect GAM dynamics, and ZF shear also can affect the GAM. These processes should be carefully examined. The stability and evolution of strongly driven GAMs may also be of interest in the context of determining fixed point and saturated states. These effects might be important when turbulence decorrelation time and GAM frequency cross-over occurs, as discussed above. We need to expand the predator-prey model to *three* predators, including mean flow shear. As denoted above, the present portrait of turbulence intensity versus temperature gradient is different from the standard L-H transition picture, because here we do not account for mean flow shearing effects on ZF/GAM shearing. Therefore mean flow is surely another player in the mode competition process. Mean flow dynamics can make "γ" self-consistent with I via transport. Stochastic forcing should be examined carefully to relate it to the physical spectrum of noise and frequency of pulsations.

Appendix A. Derivation of the minimal multiple shearing predator-prey model Eqs. (10a) and (10b).

Here we derive Eqs. (15a) and (15b) from the ZF/GAM system equations. For convenience, we change variables in Eqs. (1b)-(1d) to $(U, \sqrt{2/[(5/3+\tau)n_{eq}p_{eq}]}G, \sqrt{2}V) \rightarrow (U, G, V)$, yielding

$$\frac{\partial U}{\partial t} = (R_1(\omega) - \nu_{damp})U - \omega_{GAM}G, \tag{A.1a}$$

$$\frac{\partial G}{\partial t} = \omega_{GAM}U + \omega_{sound}V - \gamma_{LD}G, \tag{A.1b}$$

$$\frac{\partial V}{\partial t} = -\omega_{sound}G - R_3(\omega)U, \tag{A.1c}$$

where $R_1(\omega) = +(1/2)\tau_{ac,\omega}I = (1/2)\alpha_\omega I$ is response to turbulence (see Eq.(14)), which depends on mode frequency ω, $R_3(\omega) = (1/2)b\tau_{ac,\omega}I = (1/2)b\alpha_\omega I$ originates from the parallel velocity nonlinear effect $\hat{N}_{[\phi,v_\parallel]}$ in Eq. (1d), which is neglected here. $\omega_{GAM} = \sqrt{2(5/3+\tau)T_{eq}}(a/R)$, and $\omega_{sound} = \sqrt{(5/3+\tau)T_{eq}}(a/qR)$. Without turbulence drive, this system has two eigen-frequencies, namely zero (ω=0) and high frequency modes, $\omega \sim \omega_G = \sqrt{\omega_{GAM}^2 + \omega_{sound}^2}$. Correctly to estimate the shearing response of zonal flows with multiple frequencies to turbulence, we separate U by expanding Eqs. (1b) - (1d) in Fourier frequency modes and retain the zero-frequency and the high-frequency modes. We assume that the fast GAM time scale exceeds the slow transport time scale or turbulence decorrelation frequency, i.e. $\omega_G \gg \gamma_L, 1/\tau_c$. Furthermore, the GAM frequency is clearly lower than the typical drift wave frequency, i.e. $\omega_G \ll \omega_*$, so that the GAM does not violate the adiabaticity of turbulence wave action. With Fourier transformation and keeping slow time evolutions of the field $\partial_t(U_\omega, G_\omega, V_\omega)$, we obtain

$$\frac{\partial U_\omega}{\partial t} = i\omega U_\omega + (R_1(\omega) - \nu_{damp})U_\omega - \omega_{GAM}G_\omega, \tag{A.2a}$$

$$\frac{\partial G_\omega}{\partial t} = i\omega G_\omega + \omega_{GAM}U_\omega + \omega_{sound}V_\omega - \gamma_{LD}G_\omega, \tag{A.2b}$$

$$\frac{\partial V_\omega}{\partial t} = i\omega V_\omega - \omega_{sound}G_\omega. \tag{A.2c}$$

To obtain the time evolution of U_ω, we need to know those of G_ω and V_ω as well. Then we approximate the time evolutions of the three fields obeys eigenvector components corresponding those eigenfrequencies. Without any turbulence drive and dampings neglecting diagonal contributions in Eqs. (A.2a)-(A.2c), we estimate eigenvectors (U,G,V) that is $(U,G,V)=(\omega_{sound},0,-\omega_{GAM})$ for $\omega=0$ and $(U,G,V)=(\omega_{GAM}\pm i\omega_G,\omega_{sound})$ for with $\omega=\pm\omega_G$.

For the $\omega=0$ mode, from Eqs. (A2a)-(A2c), we obtain the temporal evolution of U_0 as

$$\frac{\partial U_0}{\partial t} = A_0(R(0) - \nu_{damp})U_0 = A_0(\frac{1}{2}\alpha_0 I - \nu_{damp})U_0, \tag{A.3}$$

where $A_0=(1+2q^2)^{-1}$ is a screening factor determined by the fluid model and α_0 is the coupling parameter $\alpha_0 \sim \tau_{ac,0}$. We rewrite Eq. (A.3) as the evolution of zonal flow energy, $E_0=|U_0^2|$ as

$$\frac{\partial E_0}{\partial t} = A_0(\alpha_0 I - \gamma_0)E_0, \tag{A.4}$$

where $\gamma_0=2\nu_{damp}$.

Next, for $\omega=\pm\omega_G$ modes we solve for the temporal evolution of GAM flow amplitude U_ω as

$$\frac{\partial U_\omega}{\partial t} = \frac{\omega_{GAM}^2 + i\gamma_{LD}\omega_G}{2\omega_G^2 + i\gamma_{LD}\omega_G}\left[-\frac{\gamma_{LD}\omega_G^2}{\omega_{GAM}^2 + i\gamma_{LD}\omega_G} + R(\omega_G) - \gamma_{damp}\right]U_\omega. \tag{A.5}$$

Then we obtain the evolution of GAM energy $E_\omega=|U_{+\omega}^2|+|U_{-\omega}^2|=2|U_\omega^2|=2~U_{+\omega}U_{-\omega}$, keeping in mind that the imaginary part of the factor of $U_{\pm\omega}$ is cancelled by getting the complex conjugate together.

$$\frac{\partial E_\omega}{\partial t} = \frac{2(2\omega_{GAM}^2 + \gamma_{LD}^2)}{4\omega_G^2 + \gamma_{LD}^2}\left[R(\omega_G) - 2\gamma_{damp} - \frac{2\omega_G^2\omega_{GAM}^2}{\omega_{GAM}^4 + \gamma_{LD}^2\omega_G^2}\gamma_{LD}\right]E_\omega. \tag{A.6}$$

Since $\omega_G^2 \gg \gamma_{LD}^2$ is satisfied in the edge region with $q\gg1$, γ_{LD}^2 terms in Eq. (A.6) are negligible. Thus we finally obtain the resultant description of GAM energy temporal evolution,

$$\frac{\partial E_\omega}{\partial t} = A_\omega(\alpha_\omega I - \gamma_\omega)E_\omega, \tag{A.7}$$

where $A_\omega=1-(1+2q^2)^{-1}$ is a screening factor for GAM in the fluid description, $\alpha_\omega \sim \tau_{ac,\omega}$, $\gamma_\omega=2\nu_{damp}+2(1+1/2q^2)\gamma_{LD}$ is the total damping rate for the GAM, which consists of the collisional damping effects and the screening-effect-weighted Landau damping.

Note that the evolution of U_ω, Eq. (A.5), includes higher order contributions as well as an imaginary component, which may come from mismatching of eigenfrequency and eigenvectors with dissipations from ω_G. As we find the eigen-frequency shift is the order of $O(\gamma_{LD}^2)$, the lowest order of Eq. (A6) can be kept since $\omega_G^2 \gg \gamma_{LD}^2$ is assumed.

Appendix B. Calculation of higher order wavekinetics.

In this section, we introduce the treatment of higher order perturbation of wave actions describing mode competition between ZF and GAM. We separate the perturbed wave actions by frequencies, $\omega=0,\omega_G,2\omega_G$. Thus, we rewrite the m-th perturbation terms seen in Eq. (2) as

$$\hat{N}_{k,q_r}^{(m)} = \hat{N}_{k,q_r,0}^{(m)} + \hat{N}_{k,q_r\omega_G}^{(m)} + \hat{N}_{k,q_r,2\omega_G}^{(m)}, \tag{B.1}$$

where $\hat{N}^{(m)}_{k,q_r,\omega_G}$ is the wave action with a slow dependence on $\exp(iq_r\underline{r}-i\omega_G t)$. Now we apply Eq. (4) to expansion of the higher order perturbation including the resonance as done in Eq. (5). The higher order perturbation can be described as a combination of the response with a convolution of zonal flow and the lower perturbation modes, yielding

$$\hat{N}^{(m)}_{k,q_r,\Omega} = \sum_{\substack{q_r=q'_r+q''_r \\ \Omega=\Omega'+\Omega''}} R(q_r,\Omega)k_\theta q'_r U_{q'_r,\Omega'} \frac{\partial \hat{N}^{(m-1)}_{k,q''_r,\Omega''}}{\partial k_r}. \tag{B.2}$$

As resultant beat waves from coupling of zonal flow and turbulence perturbation, perturbed modes with $2q_r$ are taken into account in calculations to the second order. Using Eq. (B.2), we yield

$$\hat{N}^{(2)}_{k,2q_r,0} = k_\theta q_r R(2q_r,0)\left(U_{q_r,0} \frac{\partial \hat{N}^{(1)}_{k,q_r,0}}{\partial k_r} + U_{q_r,\omega_G} \frac{\partial \hat{N}^{(1)}_{k,q_r,\omega_G}}{\partial k_r} \right), \tag{B.3a}$$

$$\hat{N}^{(2)}_{k,2q_r,\omega_G} = k_\theta q_r R(2q_r,\omega_G)\left(U_{q_r,0} \frac{\partial \hat{N}^{(1)}_{k,q_r,\omega_G}}{\partial k_r} + U_{q_r,\omega_G} \frac{\partial \hat{N}^{(1)}_{k,q_r,0}}{\partial k_r} \right), \tag{B.3b}$$

$$\hat{N}^{(2)}_{k,2q_r,2\omega_G} = k_\theta q_r R(2q_r,2\omega_G) U_{q_r,\omega_G} \frac{\partial \hat{N}^{(1)}_{k,q_r,\omega_G}}{\partial k_r}, \tag{B.3c}$$

followed by the third order perturbations:

$$\hat{N}^{(3)}_{k,q_r,0} = (k_\theta q_r)^2 \left\{ U^2_{q_r,0}R(q_r,0)\frac{\partial}{\partial k_r}\left[R(2q_r,0)\frac{\partial \hat{N}^{(1)}_{k,q_r,0}}{\partial k_r} \right] \right.$$

$$+ U_{q_r,0}U_{q_r,\omega_G}R(q_r,0)\frac{\partial}{\partial k_r}\left[(R(2q_r,0)+R(2q_r,\omega_G))\frac{\partial \hat{N}^{(1)}_{k,q_r,\omega_G}}{\partial k_r} \right]$$

$$+ \left. U^2_{q_r,\omega_G}R(q_r,0)\frac{\partial}{\partial k_r}\left[R(2q_r,\omega_G)\frac{\partial \hat{N}^{(1)}_{k,q_r,0}}{\partial k_r} \right] \right\}, \tag{B.4a}$$

$$\hat{N}^{(3)}_{k,q_r,\omega_G} = (k_\theta q_r)^2 \left\{ U^2_{q_r,0}R(q_r,\omega_G)\frac{\partial}{\partial k_r}\left[R(2q_r,\omega_G)\frac{\partial \hat{N}^{(1)}_{k,q_r,\omega_G}}{\partial k_r} \right] \right.$$

$$+ U_{q_r,0}U_{q_r,\omega_G}R(q_r,\omega_G)\frac{\partial}{\partial k_r}\left[[R(2q_r,0)+R(2q_r,\omega_G)]\frac{\partial \hat{N}^{(1)}_{k,q_r,0}}{\partial k_r} \right]$$

$$+ \left. U^2_{q_r,\omega_G}R(q_r,\omega_G)\frac{\partial}{\partial k_r}\left[[R(2q_r,2\omega_G)+R(2q_r,0)]\frac{\partial \hat{N}^{(1)}_{k,q_r,\omega_G}}{\partial k_r} \right] \right\}, \tag{B.4b}$$

Here we let $U_{q_r,\omega_G} = U_{q_r,-\omega_G}$ to simplify the calculation, but as discussed in Ref. [26] the relation of inward/outward propagation could change these dynamics and nonlinear parameters. These third order perturbations involve zonal flow dynamics.

Assessing the responses R($mq_r, n\omega_G$) ($m,n=0,1,2$) by autocorrelation time scale $\tau_{ac,mq,n\omega}$ defined by Eq. (9), we can estimate these higher order response with complex of ZF/GAM autocorrelation time. Therefore, from Eqs. (B.4a) and (B.4b) turbulence response to ZF and GAM up to the third order can be written as

$$R_1(0)N = -q_r^2 \frac{c^2}{B^2} \int \frac{d\underline{k}k_\theta k_r}{(1+k_\perp^2 \rho_s^2)^2} \sum_{i=1,3} \hat{N}_{k,q_r,0}^{(i)} \cong \tau_{ac,0,q_r} IU_0 \left(1 - \gamma_{00}U_0^2 - \gamma_{0\omega}U_\omega^2\right), \tag{B.5a}$$

$$R_1(\omega_G)N = -q_r^2 \frac{c^2}{B^2} \int \frac{d\underline{k}k_\theta k_r}{(1+k_\perp^2 \rho_s^2)^2} \sum_{i=1,3} \hat{N}_{k,q_r,\omega_G}^{(i)} \cong \tau_{ac,\omega_G,q_r} IU_\omega \left(1 - \gamma_{\omega 0}U_0^2 - \gamma_{\omega\omega}U_\omega^2\right), \tag{B.5b}$$

where

$$\gamma_{00} = \tau_{ac,0,q_r} \tau_{ac,0,2q_r}, \tag{B.6a}$$

$$\gamma_{0\omega} = \tau_{ac,\omega_G,q_r}(\tau_{ac,0,2q_r} + \tau_{ac,\omega_G,2q_r}) + \tau_{ac,\omega_G,q_r}\tau_{ac,0,2q_r}, \tag{B.6b}$$

$$\gamma_{\omega 0} = \tau_{ac,\omega_G,q_r}\tau_{ac,\omega_G,2q_r} + \tau_{ac,0,q_r}(\tau_{ac,\omega_G,2q_r} + \tau_{ac,0,2q_r}), \tag{B.6c}$$

$$\gamma_{00} = \tau_{ac,\omega_G,q_r}(\tau_{ac,2\omega_G,2q_r} + \tau_{ac,0,2q_r}). \tag{B.6d}$$

Assumptions we use here are following: (i) The expansion parameter is small $\varepsilon \ll 1$, (ii) the higher harmonic response R($mq_r, n\omega_G$) is characterized by the auto-correlation time $\tau_{ac,mq,n\omega}$, (iii) drift wave group velocities in the auto-coherence times can be characterized by a typical wave number, so τ_{ac} can be pulled out of the integrals over k, i.e. $\tau_{ac}(k) \cong \tau_{ac}(\overline{k})$, and (iv) the turbulence decorrelation rate $\Delta\omega$ is neglected for simplicity. Note that in Ref. [25] similar estimation of the nonlinear parameter with assumption of strong turbulence limit $\Delta\omega \gg |q_r v_{gr}|$, however we cannot neglect effects of finite frequency ω_G as well as drift wave propagation $q_r v_{gr}$. Notice that multiplication of two responses, which have pure imaginary value, exhibits minus sign! Physically, the higher order contribution corresponds to flattening effects of the distribution function of wave action through phase space diffusion as an analogy of the nonlinear Landau damping.

Furthermore we can simplify notations of Eqs. (B.6a)-(B.8d) with the definition Eq. (9). We define the autocorrelation time with ZF with $2q_r$ and ω_G by using that for ZF $\tau_{ac,ZF}(=\tau_{ac,qr,0})$ and GAM($=\tau_{ac,qr,wG}$) as

$$\frac{1}{\tau_{ac,\omega_G,2q_r}} = \frac{\varepsilon}{\tau_{ac,0,q_r}} + \frac{1}{\tau_{ac,\omega_G,q_r}}, \tag{B.7}$$

where $\varepsilon = \Delta q_{r,GAM}/\Delta q_{r,ZF}$. Finally we obtain notation of the nonlinear parameters in Eqs. (17a)-(17d).

References
[1]   Diamond P H, Itoh S-I, Itoh K, and Hahm T S 2005 *Plasma Phys. Control. Fusion* **47** R35.
[2]   Diamond P H, Liang Y-M, Carreras B A, and Terry P W 1994 *Phys. Rev. Lett.* **72** 2565.
[3]   Fujisawa A 2009 Nucl. Fusion **49** 013001.
[4]   Wagner F, Becker G, Behringer K *et al.*1982 *Phys. Rev. Lett.* **49** 1408.
[5]   Burrell K H, Ejima S, Schissel D P *et al*. 1987 Phys. Rev. Lett. **59** 1432.
[6]   Sengoku S, Funahashi A, Hasegawa M *et al*. 1987 Phys Rev. Lett. **59** 450.
[7]   Scott B. 2003 Phys. Lett. A **320** 53
[8]   Miyato N., Kishimoto Y, and Li J Q 2004 *Phys. Plasmas* **11**, 5557.
[9]   Itoh K, Hallatschek K and Itoh S-I 2005 *Plasma Phys. Control. Fusion* **47** 451.
[10]   Naulin V, Kendl A, Garcia O E *et al*. 2005 *Phys Plasmas* **12** 052515.
[11]   Hallatschek K 2007 *Plasma Phys. Control. Fusion* **49** B137.

[12] C. Holland, Tynan G R, Fonck R J *et al*. 2007 *Phys Plasmas* **14** 056112.
[13] Guzdar P N, Kleva R G, Chakrabarti N *et al.* 2009 *Phys. Plasmas* **16** 052514.
[14] McKee G R, Gohil P, Schlossberg D J *et al*. 2009 *Nucl. Fusion* **49** 115016.
[15] Conway et al. in Fusion Energy 2010 (Proc. 23rd Int. Conf. Daejeon, 2010) (Vienna: IAEA) CD-ROM file EXC/7-1 and   http://www-naweb.iaea.org/napc/physics/FEC/FEC2010/html/index.htm
[16] Zhao K J et al. in Fusion Energy 2010 (Proc. 23rd Int. Conf. Daejeon, 2010) (Vienna: IAEA) CD-ROM file EXC/7-3 and http://www-naweb.iaea.org/napc/physics/FEC/FEC2010/html/index.htm
[17] Zhao K J, Dong J Q, Yan L W *et al*. 2010 *Plasma Phys. Control. Fusion* **52** 124008.
[18] Kim E J and Diamond P H 2003 *Phys. Rev. Lett.* **90**, 185006.
[19] Miki K, Kishimoto Y, Miyato N, and Li J Q 2007 *Phys. Rev. Lett.* **99**, 145003.
[20] Miki K, Kishimoto Y, Miyato N, and Li J Q 2008 *J. Phys.: Conf. Ser.* **123**, 012028.
[21] Miki K and Diamond P H 2010 *Phys. Plasmas* **17**, 032309.
[22] Hahm T.S., Beer M A, Lin Z *et al.* 1999 Phys. Plasmas **6** 922.
[23] Diamond P H, Itoh S-I, and Itoh K 2010 *Modern Plasma Physics Vol. 1: Physical Kinetics of Turbulent Plasmas* (New York: Cambridge University Press).
[24] May R M, 1973 *Stability and Complexity in Model Ecosystems* (Princeton: Princeton University Press).
[25] Itoh K, Hallatschek K, Itoh S-I *et al*. 2005 *Phys. Plasmas* **12**, 062303.
[26] Sasaki M, Itoh K, Ejiri A, and Takase Y 2009 *Plasma Phys. Control. Fusion* **51**, 085002.
[27] Hirsch M W, Smale S, and Devaney R L 2004 *Differential Equations, Dynamical Systems, and an Introduction to Chaos* (London: Elsevier Academic Press).
[28] Hinton F L 1991 *Phys. Fluids B* **3**, 696.
[29] Itoh S-I, Itoh K, and Toda S 2003 *Plasma Phys. Control. Fusion* **45** 823.
[30] Malkov M A and Diamond P H 2009 *Phys. Plasmas* **16** 012504.
[31] Pikovsky A, Rosenblum M, and Kurths J, 2001 *Synchronization, A universal concept in nonlinear sciences* (New York: Cambridge University Press).
[32] Miki K., "*Transport Dynamics Associated with Geodesic Acoustic Mode near the Critical Gradient Regime in Tokamak Plasmas",* 2008 Ph.D Thesis, Kyoto University.
[33] Barbay S, Giacomelli G, and Marin F 2000 *Phys. Rev. E* **61** 157.
[34] Laval J-P, Dubrulle B, and Nazarenko S 2001 Phys. Fluids **13** 1995.
[35] Dimits A M, Bateman G, Beer M A *et al.* 2000 *Phys. Plasmas* **7** 969.